View metadata, citation and similar papers at core.ac.uk

brought to you by CORE

provided by Digital.CSIC

Enhanced excitonic effects in the energy loss spectra of LiF and Ar at large momentum transfer

This content has been downloaded from IOPscience. Please scroll down to see the full text.

2012 New J. Phys. 14 053052

(http://iopscience.iop.org/1367-2630/14/5/053052)

View the table of contents for this issue, or go to the journal homepage for more

Download details:

IP Address: 161.111.180.191
This content was downloaded on 11/04/2014 at 13:03

Please note that terms and conditions apply.

New Journal of Physics
The open-access journal for physics

Enhanced excitonic effects in the energy loss spectra of LiF and Ar at large momentum transfer

S Sharma[1,3], J K Dewhurst[1], A Sanna[1], A Rubio[2] and E K U Gross[1]

[1] Max-Planck-Institut für Mikrostrukturphysik, Weinberg 2, D-06120 Halle, Germany

[2] Nano-Bio Spectroscopy group and ETSF Scientific Development Centre, Centro de Física de Materiales CSIC-UPV/EHU-MPC and DIPC, Universidad del País Vasco UPV/EHU, Avenida de Tolosa 72, E-20018 San Sebastian, Spain

E-mail: sharma@mpi-halle.mpg.de

New Journal of Physics **14** (2012) 053052 (8pp)
Received 2 April 2012
Published 31 May 2012
Online at http://www.njp.org/
doi:10.1088/1367-2630/14/5/053052

Abstract. It is demonstrated that the bootstrap kernel [1] for finite values of $\mathbf{q}$ crucially depends upon the matrix character of the kernel and gives results of the same good quality as in the $\mathbf{q} \to 0$ limit. The bootstrap kernel is further used to study the electron loss as well as the dielectric tensor for Si, LiF and Ar for various values of $\mathbf{q}$. The results show that the excitonic effects in LiF and Ar are enhanced for values of $\mathbf{q}$ away from the Γ-point. The reason for this enhancement is the interaction between the exciton and high-energy inter-band electron–hole transitions. This fact is validated by calculating the absorption spectra under the influence of an external electric field. The electron energy loss spectra are shown to change dramatically as a function of $\mathbf{q}$.

One of the promising routes for tailoring electro-magnetic interactions in systems is to make use of excitons—excitonic condensation [2, 3], exciton–plasmon interaction [4, 5] and a strong coupling of excitons with other inter-band optical transitions. A number of applications of excitonic manipulation have found their way into surface physics, nano-structures and nano-tubes. Extended solids, however, have not been treated as serious candidates for such effects. This is mainly due to the fact that excitonic effects are in general (but not exclusively) stronger in lower-dimensional systems [6].

[3] Author to whom any correspondence should be addressed.

© IOP Publishing Ltd and Deutsche Physikalische Gesellschaft

As to solids, much of the attention of excitonic physics has been focused on the determination of optical absorption spectra (in the long-wavelength ($q \to 0$) limit). The determination of optical absorption spectra in this limit requires an accurate description of electron–hole effects, which in turn requires a computationally expensive many-body treatment at the level of the Bethe–Salpeter equation (BSE) [7–14]. Alternatively, this electron–hole physics can also be effectively treated using time-dependent density functional theory (TDDFT) [15]. However, there exist only a few exchange-correlation (xc) kernels within TDDFT that are capable of accurately describing the excitonic effects arising from strong electron–hole interactions: the computationally demanding but accurate nano-quanta kernel [16–18] that is derived from the BSE, the long-range corrected (LRC) kernel [16, 19, 20] that has the form $\alpha/|q|^2$ (with α being a system-dependent external parameter) and the recently proposed bootstrap kernel [1]. The main feature that makes these kernels capable of accurately treating the absorption spectra (in the $q \to 0$ limit) is their $1/|q|^2$ dependence [21], a feature necessary for capturing the electron–hole physics.

In contrast to this, the dielectric tensor and the electron energy loss spectra (EELS) at finite values of $\mathbf{q}$ (away from the Γ-point) are known to be accurately treated [22, 23] by the adiabatic local density approximation (ALDA) ([24] and references therein), which does not have the $1/|q|^2$ dependence. This then raises an interesting question about the validity of the kernels which accurately treat the $\mathbf{q} \to 0$, for finite values of $\mathbf{q}$.

In this work, the EELS and the imaginary part of the dielectric tensor for Si, diamond, LiF and Ar are calculated using the bootstrap kernel [1]. This choice is motivated by the fact that the bootstrap kernel is computationally undemanding and does not depend upon any system-dependent parameters. For prototypical materials with bound electron–hole pairs, LiF and Ar, there exists a strong coupling between excitons with high-energy inter-band transitions (ITs), which leads to strong excitonic effects away from the Γ-point. This coupling provides a useful handle to manipulate the excitonic physics, since ITs can easily be modified by changing the external parameters such as pressure and/or electric field.

The bootstrap xc kernel within TDDFT for calculating the linear response reads

$$f_{\mathrm{xc}}^{\mathrm{boot}}(\mathbf{q},\omega) = -\frac{\varepsilon^{-1}(\mathbf{q},\omega=0)v(\mathbf{q})}{\varepsilon_0^{00}(\mathbf{q},\omega=0)-1} = \frac{\varepsilon^{-1}(\mathbf{q},\omega=0)}{\chi_0^{00}(\mathbf{q},\omega=0)} \tag{1}$$

with

$$\begin{aligned}\varepsilon^{-1}(\mathbf{q},\omega) &= 1 + v(\mathbf{q})\chi(\mathbf{q},\omega) \\ &= 1 + \chi_0(\mathbf{q},\omega)v(\mathbf{q})\left[1 - (v(\mathbf{q}) + f_{\mathrm{xc}}^{\mathrm{boot}}(\mathbf{q},\omega))\chi_0(\mathbf{q},\omega)\right]^{-1},\end{aligned} \tag{2}$$

where v is the bare Coulomb potential, χ_0 is the response function of the non-interacting Kohn–Sham system and $\varepsilon_0(\mathbf{q},\omega) \equiv 1 - v(\mathbf{q})\chi_0(\mathbf{q},\omega)$ is the dielectric function in the random phase approximation (RPA). All these quantities are matrices in the basis of reciprocal lattice vectors $\mathbf{G}$. The head of the matrix ε, i.e. the $\mathbf{G} = \mathbf{G}' = 0$ component, is what is measured (either directly or indirectly) experimentally.

Equations (1) and (2) are solved self-consistently. The χ_0 in equation (2) is calculated using an approximate ground state xc functional: the local density approximation (LDA). To overcome the shortcomings of such an approximation, we replace the χ_0 by a response function obtained from the scissors-corrected LDA. This has the advantage that χ_0, and consequently χ, has the correct gap to begin with (for details see [1]). All the calculations are performed using

the full-potential linearized augmented plane wave method [25], implemented within the Elk code [26]. A k-point mesh of $25 \times 25 \times 25$ is used to ensure convergence.

With a view to studying the excitonic properties of solids for any value of $\mathbf{q}$, we first show that the bootstrap kernel for finite values of $\mathbf{q}$ leads to accurate results. This is demonstrated in figure 1, which compiles the results for the dielectric response and EELS of a small-band-gap insulator, Si, a medium-band-gap insulator, diamond, and a large-band-gap insulator, LiF. The choice of these materials is motivated by the abundance of available experimental data and because they have been used as prototypical test cases for the influence of many-body corrections.

In the upper two panels of figure 1 are presented the results for $\varepsilon(\mathbf{q}, \omega)$ of Si. The results obtained using the bootstrap kernel are compared with the results obtained using the ALDA and with the experimental data. It is clear that as far as the imaginary part of the dielectric tensor is concerned, the bootstrap kernel (treated as a full matrix in reciprocal space) gives results in good agreement with experiments. Interestingly, for small frequencies the results obtained using the bootstrap kernel give an upper bound to the experimental data, while the results obtained using the ALDA give a lower bound. The RPA results (also shown in figure 1), as expected, totally miss the excitonic physics, which in this case shows up as the shifting of the spectral weight to lower frequencies.

In the $\mathbf{q} \to 0$ limit, the $\mathbf{G} = \mathbf{G}' = 0$ component of f_{xc} is the most important one and hence the bootstrap procedure can be thought of as a self-consistent method for obtaining the system-dependent parameter α of the LRC. For finite values of $\mathbf{q}$ the matrix character of f_{xc} is crucial and the bootstrap kernel is significantly different from the LRC kernel. The importance of including higher $\mathbf{G}$ vectors in f_{xc} is demonstrated in figure 1; the results for Si show that the dielectric function obtained using only the $\mathbf{G} = \mathbf{G}' = 0$ component of f_{xc} is much higher in magnitude and in relatively poor agreement with the experimental data. EELS corresponds to the negative of the imaginary part of $\varepsilon^{-1}_{00}(\mathbf{q}, \omega)$, where 00 stands for the $\mathbf{G} = \mathbf{G}' = 0$ component of the dielectric tensor. The lower panel of figure 1 contains the results for the EELS of LiF and diamond. Three different values of $\mathbf{q}$ in the Γ–X-direction are presented for LiF. Within the first Brillouin zone (BZ) the experimental data and BSE results show three main peaks that are reproduced well by the bootstrap kernel. On going from 0.23 to 0.48 ΓX the plasmonic peak at 25 eV decreases in magnitude, a feature that is again well captured by the bootstrap kernel. Experiments, BSE and bootstrap results show that outside the first BZ (for $\mathbf{q} = 1.50\Gamma X$) EELS is highly suppressed. These results indicate that the bootstrap kernel captures the change in $-\mathrm{Im}[\varepsilon^{-1}]$ as a function of $\mathbf{q}$ very well. We note, however, that the magnitude of the peaks is slightly overestimated by the bootstrap kernel and, for small energies, the peaks are blue-shifted by $\sim$1 eV compared to experiment. This shifting of the excitonic peaks to higher frequencies and the overestimation of their magnitude were also a feature of the absorption spectra in the long-wavelength limit.

For diamond, the magnitude of the EELS obtained using the bootstrap kernel is overestimated compared to the experiment. A similar overestimation is also seen in the BSE results [27]. In fact, we find that the results obtained using the bootstrap kernel are in very good agreement with the BSE results.

As in the case of Si, the RPA results are shifted to higher frequencies compared to the BSE and experimental data for both LiF and diamond. The results obtained using the ALDA for LiF and diamond are also shown in figure 1. The ALDA results are an improvement over RPA. However, the ALDA results disagree with the BSE data for large values of $\mathbf{q}$.

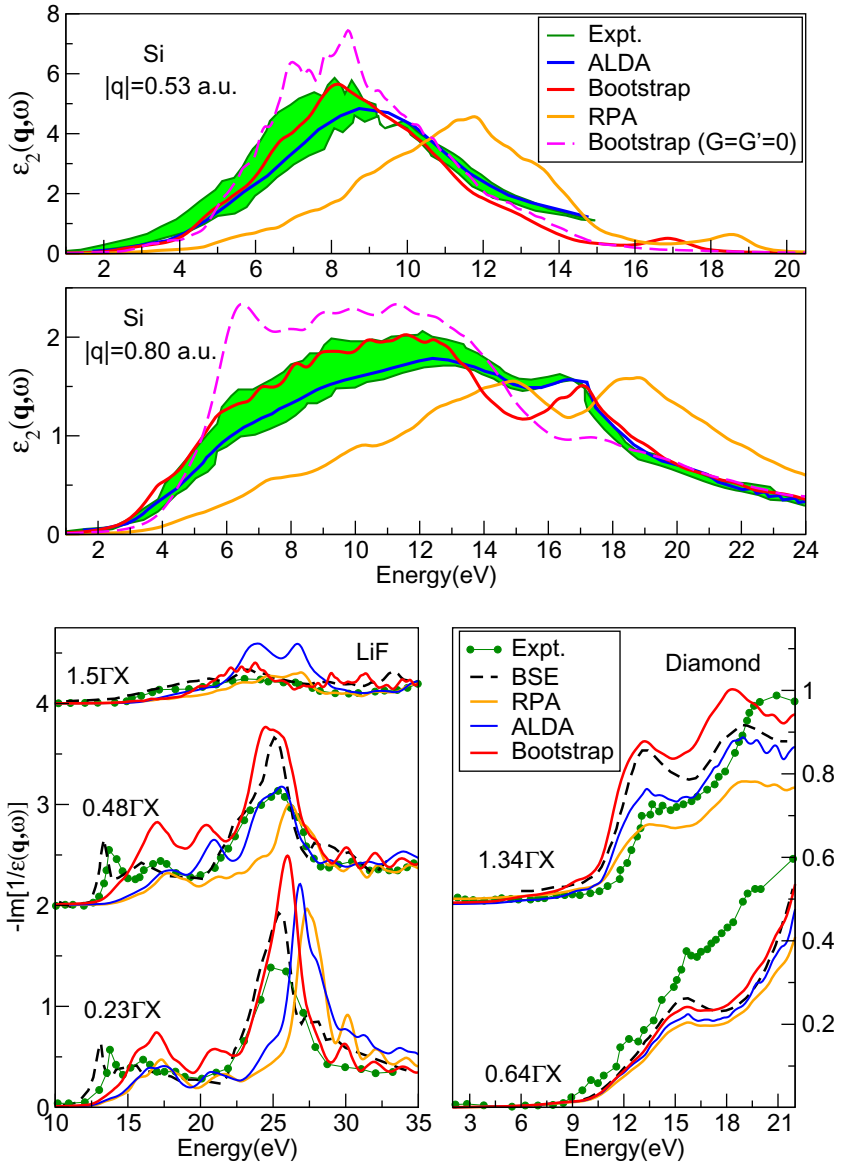

Figure 1. Upper two panels: the imaginary part of the dielectric tensor as a function of energy in eV for Si. The results obtained using the bootstrap kernel, RPA and ALDA are compared with the experimental data of [23]. The top panel contains the results for $|\mathbf{q}| = 0.53$ au and the middle panel those for $|\mathbf{q}| = 0.80$ au parallel to the [111] direction. The bootstrap results are obtained in two different ways: (red line) the kernel is a full matrix in the reciprocal space with $|\mathbf{G}|_{\max} = 4$ au and (pink dotted line) only the head of the kernel is used, i.e. $|\mathbf{G}|_{\max} = 0$ au. The bottom panel contains the results for the EELS for different values of $\mathbf{q}$ (indicated in the figure) as a function of energy in eV for LiF and diamond. The results obtained using the bootstrap kernel are shown by the full line, the experimental data (from [27]) with dots, the BSE results (also taken from [27]) with the dashed line and the ALDA results with thin (blue) line. The results for different values of $\mathbf{q}$ are shifted vertically for clarity.

It is apparent from the above examples that the bootstrap results for values of $\mathbf{q}$ away from the Γ-point show the same good agreement with experiments as those in the $\mathbf{q} \to 0$ limit. With this in hand we can now use the bootstrap kernel to study the excitonic effects in various directions in the BZ.

In figure 2, the results for $\varepsilon(\mathbf{q}, \omega)$ are shown for LiF and Ar for various values of $\mathbf{q}$. The upper panel contains the results for LiF in the Γ–L–X-direction.[4] It is immediately clear from this that the excitonic peak in LiF becomes stronger (spectral weight moves to lower frequency) away from the Γ-point; on going from Γ to L, the excitonic peak ($\sim$13–14 eV) increases in magnitude and, at the same time, the IT peak $\sim$20 eV diminishes and moves to lower frequencies (from 20 to 18 eV). In the L–X-direction the excitonic and IT peaks remain almost the same.

Similar results are also seen for Ar; on going from Γ to L, the spectral weight moves towards the excitonic peak ($\sim$12 eV), which becomes stronger and shifts to lower frequencies. This is accompanied by a steady diminishing of the IT peak around 18 eV. Beyond $0.6\Gamma L$, both the excitonic and the IT peaks are unchanged. The RPA for both LiF and Ar misses this excitonic physics for all values of $\mathbf{q}$.

The above results point towards a strong coupling between the excitonic and the IT peaks; as the excitonic peak gains weight, the IT peak diminishes. This observation could be used in the future to tune excitonic effects via manipulation of ITs. In order to validate this hypothesis we have performed calculations of the $\mathbf{q} \to 0$ absorption spectrum for LiF in the presence of an external electric field. This field is an artifice used to lift the degeneracy and split the bands[5]. This split in the bands causes the IT peak at 20 eV to diminish and move to lower energies. The excitonic peak gains weight (spectral weight moves to lower energy) and the results for ε in the $\mathbf{q} \to 0$ limit closely resemble those of the L-point (see the top panel of figure 2). Such a tuning of the excitons has been performed before: a coupling of excitons and surface plasmons was used to enhance the excitonic effects in low-dimensional systems [4, 5, 28].

At this point it is important to mention that this suppression of the IT peak as a function of $\mathbf{q}$ is also present in the ALDA results. This suppression of the IT peak leads to a redistribution of the spectral weight—a natural consequence of the optical sum rules. However, since the excitonic peak is not captured by ALDA (or RPA), one cannot observe coupling of the IT and excitonic peaks, making the physics of excitonic tuning and enhancement inaccessible.

$\varepsilon_{00}^{-1}(\mathbf{q}, \omega)$ is an important quantity, not just because it can be directly compared to experiments, but also because it is required for an accurate determination of the screened Coulomb interaction, $W = \varepsilon^{-1} v$. In Hedin's theoretical foundation of many-body perturbation theory the effective interaction, W, is a crucial concept. It is needed as an essential ingredient if one wishes to sum Feynman diagrams to obtain the Green's function of a system [7, 9]. In figure 3, we present the results for the EELS of LiF as a function of $\mathbf{q}$ and frequency. The EELS changes dramatically as a function of $\mathbf{q}$; the peak at 16 eV gains height on moving in the Γ–L-direction (upper panel), while at the same time the peak at 25 eV diminishes in magnitude and broadens. This leads to the EELS for $\mathbf{q} \to 0$ being significantly different from that at $\mathbf{q} = [0.5, 0.5, 0.5]$. A similar sharpening of the peak at 16 eV is also seen in the L–X-direction (lower panel); a broad double peak at $\sim$18 eV changes to one sharp peak at 16 eV and

[4] Γ–L–X = [0, 0, 0]–[0.5, 0.5, 0.5]–[0.5, 0.5, 0].

[5] A constant field of sawtooth shape is added. The scalar potential corresponding to this is calculated and added to the full Kohn–Sham potential. The sawtooth shape implies that the applied electric field abruptly ends at the unit-cell boundary, making this field unphysical in nature.

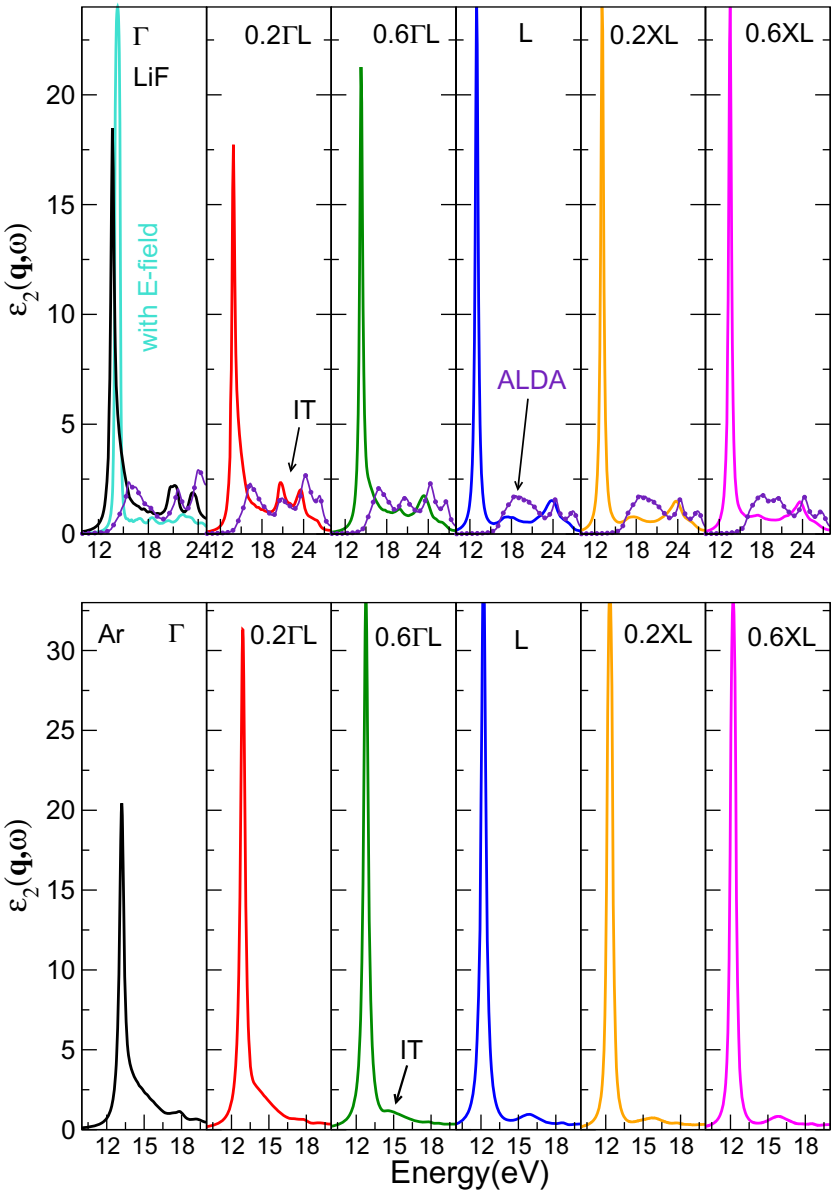

Figure 2. The dielectric tensor obtained using the bootstrap kernel as a function of energy in eV. The upper panel contains the results for LiF and the lower panel for Ar in the Γ–L–X-direction. The upper leftmost panel also contains the results at the Γ-point for LiF exposed to an external electric field. For LiF, results obtained using the ALDA are also presented in the upper panel.

a small shoulder at ∼20 eV. In the L–X-direction (unlike the Γ–L) the peak at 25 eV stays almost unchanged as a function of $\mathbf{q}$. Similar strong changes in EELS as a function of $\mathbf{q}$, in the Γ–U-direction for LiF, have been reported previously in [29].

The RPA and ALDA results (also shown in figure 3) not only miss the low-energy excitonic effects [29], but also show very little variation as a function of $\mathbf{q}$ in both the Γ–L and X–L directions. Most many-body calculations use RPA dielectric functions to screen the Coulomb

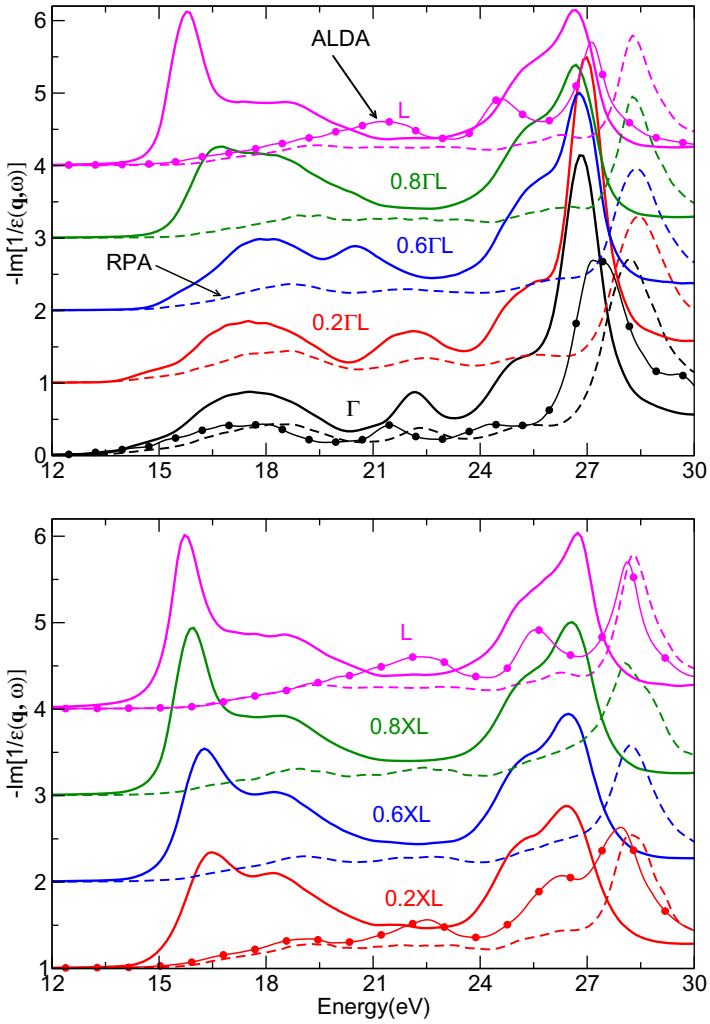

Figure 3. Electron energy loss spectrum ($-\mathrm{Im}[\varepsilon_{00}^{-1}(\mathbf{q}, \omega)]$) in arbitrary units as a function of energy in eV for LiF. The results obtained using the bootstrap kernel are shown with full lines, the results obtained using the RPA with dashed lines and the results obtained using ALDA with dotted lines. The upper panel shows the results in the Γ–L-direction and the lower panel those in the X–L-direction. The results for various values of $\mathbf{q}$ are shifted vertically for clarity.

potential. However, it is clear from the present study that RPA dielectric functions can strongly differ from those which properly include electron–hole physics. TDDFT with the bootstrap kernel is a computationally efficient method to accurately determine $\varepsilon^{-1}(\mathbf{q}, \omega)$ for use in many-body perturbation theory [29].

To summarize, in this work it is demonstrated that the results obtained using the bootstrap kernel for finite values of $\mathbf{q}$ have the same accuracy as those in the $\mathbf{q} \to 0$ limit. We use this kernel to make predictions that in the prototypical materials LiF and Ar excitonic effects are enhanced *away* from Γ. This enhancement is attributed to the interaction between the exciton and other high-energy ITs. This observation is reinforced by the application of an external electric field and noting an inverse proportionality in strength between the inter-band and

excitonic peaks. It is further demonstrated that the EELS also changes dramatically as a function of **q**. This strong change in EELS is missing within the RPA, and hence it is highly desirable to use a TDDFT dielectric function for screening the Coulomb interaction as the input for many-body perturbation theory.

Acknowledgments

AR acknowledges funding from the European Research Council Advanced Grant DYNamo (ERC-2010-AdG -Proposal no. 267374), Spain (FIS2010-21282-C02-01 and PIB2010US-00652), Grupos Consolidados UPV/EHU del Gobierno Vasco (IT-319-07) and ACI-Promociona (ACI2009-1036).

References

[1] Sharma S, Dewhurst J K, Sanna A and Gross E K U 2011 *Phys. Rev. Lett.* **107** 186401
[2] Keldysh L V and Kopaev Y V 1964 *Fiz. Tverd. Tela* **6** 2781
[3] Eisenstein J P and MacDonald A H 2004 *Nature* **432** 691
[4] Bondarev I V, Woods L M and Tatur K 2009 *Phys. Rev.* B **80** 085407
[5] Bellessa J, Bonnand C, Plenet J C and Mugnier J 2004 *Phys. Rev. Lett.* **93** 036404
[6] Wirtz L, Marini A and Rubio A 2006 *Phys. Rev. Lett.* **96** 126104
[7] Hanke W 1978 *Adv. Phys.* **27** 278
[8] Onida G *et al* 1995 *Phys. Rev. Lett.* **75** 818
[9] Onida G *et al* 2002 *Rev. Mod. Phys.* **74** 601
[10] Rohlfing M and Louie S G 1998 *Phys. Rev. Lett.* **81** 2312
[11] Laskowski R and Christensen N E 2007 *Phys. Status Solidi* b **244** 17
[12] Hahn P H *et al* 2005 *Phys. Status Solidi* b **242** 2720
[13] Bechstedt F *et al* 2005 *Phys. Rev.* B **72** 245114
[14] Galamic-Mulaomerovic S and Patterson C H 2005 *Phys. Rev.* B **72** 035127
[15] Runge E and Gross E K U 1984 *Phys. Rev. Lett.* **52** 997
[16] Reining L *et al* 2002 *Phys. Rev. Lett.* **88** 066404
[17] Marini A, Del Sole R and Rubio A 2003 *Phys. Rev. Lett.* **91** 256402
[18] Sottile F *et al* 2003 *Phys. Rev. Lett.* **91** 056402
[19] Botti S *et al* 2004 *Phys. Rev.* B **69** 155112
[20] Botti S *et al* 2005 *Phys. Rev.* B **72** 125203
[21] Ghosez P *et al* 1997 *Phys. Rev.* B **56** 12811
[22] Botti S *et al* 2007 *Rep. Prog. Phys.* **70** 357
[23] Weissker H-C, Serrano J, Huotari S, Luppi E, Cazzaniga M, Bruneval F, Sottile F, Monaco G, Olevano V and Reining L 2010 *Phys. Rev.* B **81** 085104
[24] Gross E K U, Dobson F J and Petersilka M 1996 *Top. Curr. Chem.* **181** 81
[25] Singh D J 1994 *Planewaves Pseudopotentials and the LAPW Method* (Boston, MA: Kluwer)
[26] 2004 http://elk.sourceforge.net
[27] Caliebe W A, Soininen J A, Shirley E L, Kao C-C and Hämäläinen K 2000 *Phys. Rev. Lett.* **84** 3907
[28] Attaccalite C, Bockstedte M, Marini A, Rubio A and Wirtz L 2011 *Phys. Rev.* B **83** 144115
[29] Marini A and Rubio A 2004 *Phys. Rev.* B **70** 081103